August 2008

Search for Decay of a Fermiophobic Higgs Boson $h_f \rightarrow \gamma\gamma$ with the D0 Detector at $\sqrt{s}$ = 1.96 TeV

V. M. Abazov
Joint Institute for Nuclear Research, Dubna, Russia

Kenneth A. Bloom
University of Nebraska-Lincoln, kenbloom@unl.edu

Gregory Snow
University of Nebraska-Lincoln, gsnow1@unl.edu

DØ Collaboration

Search for Decay of a Fermiophobic Higgs Boson $h_f \to \gamma\gamma$ with the D0 Detector at $\sqrt{s} = 1.96$ TeV

V. M. Abazov,[36] B. Abbott,[75] M. Abolins,[65] B. S. Acharya,[29] M. Adams,[51] T. Adams,[49] E. Aguilo,[6] S. H. Ahn,[31] M. Ahsan,[59] G. D. Alexeev,[36] G. Alkhazov,[40] A. Alton,[64,*] G. Alverson,[63] G. A. Alves,[2] M. Anastasoaie,[35] L. S. Ancu,[35] T. Andeen,[53] S. Anderson,[45] B. Andrieu,[17] M. S. Anzelc,[53] M. Aoki,[50] Y. Arnoud,[14] M. Arov,[60] M. Arthaud,[18] A. Askew,[49] B. Åsman,[41] A. C. S. Assis Jesus,[3] O. Atramentov,[49] C. Avila,[8] C. Ay,[24] F. Badaud,[13] A. Baden,[61] L. Bagby,[50] B. Baldin,[50] D. V. Bandurin,[59] P. Banerjee,[29] S. Banerjee,[29] E. Barberis,[63] A.-F. Barfuss,[15] P. Bargassa,[80] P. Baringer,[58] J. Barreto,[2] J. F. Bartlett,[50] U. Bassler,[18] D. Bauer,[43] S. Beale,[6] A. Bean,[58] M. Begalli,[3] M. Begel,[73] C. Belanger-Champagne,[41] L. Bellantoni,[50] A. Bellavance,[50] J. A. Benitez,[65] S. B. Beri,[27] G. Bernardi,[17] R. Bernhard,[23] I. Bertram,[42] M. Besançon,[18] R. Beuselinck,[43] V. A. Bezzubov,[39] P. C. Bhat,[50] V. Bhatnagar,[27] C. Biscarat,[20] G. Blazey,[52] F. Blekman,[43] S. Blessing,[49] D. Bloch,[19] K. Bloom,[67] A. Boehnlein,[50] D. Boline,[62] T. A. Bolton,[59] G. Borissov,[42] T. Bose,[77] A. Brandt,[78] R. Brock,[65] G. Brooijmans,[70] A. Bross,[50] D. Brown,[81] N. J. Buchanan,[49] D. Buchholz,[53] M. Buehler,[81] V. Buescher,[22] V. Bunichev,[38] S. Burdin,[42,†] S. Burke,[45] T. H. Burnett,[82] C. P. Buszello,[43] J. M. Butler,[62] P. Calfayan,[25] S. Calvet,[16] J. Cammin,[71] W. Carvalho,[3] B. C. K. Casey,[50] H. Castilla-Valdez,[33] S. Chakrabarti,[18] D. Chakraborty,[52] K. Chan,[6] K. M. Chan,[55] A. Chandra,[48] F. Charles,[19,**] E. Cheu,[45] F. Chevallier,[14] D. K. Cho,[62] S. Choi,[32] B. Choudhary,[28] L. Christofek,[77] T. Christoudias,[43] S. Cihangir,[50] D. Claes,[67] Y. Coadou,[6] M. Cooke,[80] W. E. Cooper,[50] M. Corcoran,[80] F. Couderc,[18] M.-C. Cousinou,[15] S. Crépé-Renaudin,[14] D. Cutts,[77] M. Ćwiok,[30] H. da Motta,[2] A. Das,[45] G. Davies,[43] K. De,[78] S. J. de Jong,[35] E. De La Cruz-Burelo,[64] C. De Oliveira Martins,[3] J. D. Degenhardt,[64] F. Déliot,[18] M. Demarteau,[50] R. Demina,[71] D. Denisov,[50] S. P. Denisov,[39] S. Desai,[50] H. T. Diehl,[50] M. Diesburg,[50] A. Dominguez,[67] H. Dong,[72] L. V. Dudko,[38] L. Duflot,[16] S. R. Dugad,[29] D. Duggan,[49] A. Duperrin,[15] J. Dyer,[65] A. Dyshkant,[52] M. Eads,[67] D. Edmunds,[65] J. Ellison,[48] V. D. Elvira,[50] Y. Enari,[77] S. Eno,[61] P. Ermolov,[38] H. Evans,[54] A. Evdokimov,[73] V. N. Evdokimov,[39] A. V. Ferapontov,[59] T. Ferbel,[71] F. Fiedler,[24] F. Filthaut,[35] W. Fisher,[50] H. E. Fisk,[50] M. Fortner,[52] H. Fox,[42] S. Fu,[50] S. Fuess,[50] T. Gadfort,[70] C. F. Galea,[35] E. Gallas,[50] C. Garcia,[71] A. Garcia-Bellido,[82] V. Gavrilov,[37] P. Gay,[13] W. Geist,[19] D. Gelé,[19] C. E. Gerber,[51] Y. Gershtein,[49] D. Gillberg,[6] G. Ginther,[71] N. Gollub,[41] B. Gómez,[8] A. Goussiou,[82] P. D. Grannis,[72] H. Greenlee,[50] Z. D. Greenwood,[60] E. M. Gregores,[4] G. Grenier,[20] Ph. Gris,[13] J.-F. Grivaz,[16] A. Grohsjean,[25] S. Grünendahl,[50] M. W. Grünewald,[30] F. Guo,[72] J. Guo,[72] G. Gutierrez,[50] P. Gutierrez,[75] A. Haas,[70] N. J. Hadley,[61] P. Haefner,[25] S. Hagopian,[49] J. Haley,[68] I. Hall,[65] R. E. Hall,[47] L. Han,[7] K. Harder,[44] A. Harel,[71] R. Harrington,[63] J. M. Hauptman,[57] R. Hauser,[65] J. Hays,[43] T. Hebbeker,[21] D. Hedin,[52] J. G. Hegeman,[34] J. M. Heinmiller,[51] A. P. Heinson,[48] U. Heintz,[62] C. Hensel,[58] K. Herner,[72] G. Hesketh,[63] M. D. Hildreth,[55] R. Hirosky,[81] J. D. Hobbs,[72] B. Hoeneisen,[12] H. Hoeth,[26] M. Hohlfeld,[22] S. J. Hong,[31] S. Hossain,[75] P. Houben,[34] Y. Hu,[72] Z. Hubacek,[10] V. Hynek,[9] I. Iashvili,[69] R. Illingworth,[50] A. S. Ito,[50] S. Jabeen,[62] M. Jaffré,[16] S. Jain,[75] K. Jakobs,[23] C. Jarvis,[61] R. Jesik,[43] K. Johns,[45] C. Johnson,[70] M. Johnson,[50] A. Jonckheere,[50] P. Jonsson,[43] A. Juste,[50] E. Kajfasz,[15] A. M. Kalinin,[36] J. M. Kalk,[60] S. Kappler,[21] D. Karmanov,[38] P. A. Kasper,[50] I. Katsanos,[70] D. Kau,[49] V. Kaushik,[78] R. Kehoe,[79] S. Kermiche,[15] N. Khalatyan,[50] A. Khanov,[76] A. Kharchilava,[69] Y. M. Kharzheev,[36] D. Khatidze,[70] T. J. Kim,[31] M. H. Kirby,[53] M. Kirsch,[21] B. Klima,[50] J. M. Kohli,[27] J.-P. Konrath,[23] V. M. Korablev,[39] A. V. Kozelov,[39] J. Kraus,[65] D. Krop,[54] T. Kuhl,[24] A. Kumar,[69] A. Kupco,[11] T. Kurča,[20] J. Kvita,[9] F. Lacroix,[13] D. Lam,[55] S. Lammers,[70] G. Landsberg,[77] P. Lebrun,[20] W. M. Lee,[50] A. Leflat,[38] J. Lellouch,[17] J. Leveque,[45] J. Li,[78] L. Li,[48] Q. Z. Li,[50] S. M. Lietti,[5] J. G. R. Lima,[52] D. Lincoln,[50] J. Linnemann,[65] V. V. Lipaev,[39] R. Lipton,[50] Y. Liu,[7] Z. Liu,[6] A. Lobodenko,[40] M. Lokajicek,[11] P. Love,[42] H. J. Lubatti,[82] R. Luna,[3] A. L. Lyon,[50] A. K. A. Maciel,[2] D. Mackin,[80] R. J. Madaras,[46] P. Mättig,[26] C. Magass,[21] A. Magerkurth,[64] P. K. Mal,[82] H. B. Malbouisson,[3] S. Malik,[67] V. L. Malyshev,[36] H. S. Mao,[50] Y. Maravin,[59] B. Martin,[14] R. McCarthy,[72] A. Melnitchouk,[66] L. Mendoza,[8] P. G. Mercadante,[5] M. Merkin,[38] K. W. Merritt,[50] A. Meyer,[21] J. Meyer,[22,§] T. Millet,[20] J. Mitrevski,[70] J. Molina,[3] R. K. Mommsen,[44] N. K. Mondal,[29] R. W. Moore,[6] T. Moulik,[58] G. S. Muanza,[20] M. Mulders,[50] M. Mulhearn,[70] O. Mundal,[22] L. Mundim,[3] E. Nagy,[15] M. Naimuddin,[50] M. Narain,[77] N. A. Naumann,[35] H. A. Neal,[64] J. P. Negret,[8] P. Neustroev,[40] H. Nilsen,[23] H. Nogima,[3] S. F. Novaes,[5] T. Nunnemann,[25] V. O'Dell,[50] D. C. O'Neil,[6] G. Obrant,[40] C. Ochando,[16] D. Onoprienko,[59] N. Oshima,[50] N. Osman,[43] J. Osta,[55] R. Otec,[10] G. J. Otero y Garzón,[50] M. Owen,[44] P. Padley,[80] M. Pangilinan,[77] N. Parashar,[56] S.-J. Park,[71] S. K. Park,[31] J. Parsons,[70] R. Partridge,[77] N. Parua,[54] A. Patwa,[73] G. Pawloski,[80] B. Penning,[23] M. Perfilov,[38] K. Peters,[44] Y. Peters,[26] P. Pétroff,[16] M. Petteni,[43] R. Piegaia,[1] J. Piper,[65] M.-A. Pleier,[22] P. L. M. Podesta-Lerma,[33,‡] V. M. Podstavkov,[50] Y. Pogorelov,[55] M.-E. Pol,[2] P. Polozov,[37] B. G. Pope,[65] A. V. Popov,[39] C. Potter,[6] W. L. Prado da Silva,[3] H. B. Prosper,[49] S. Protopopescu,[73] J. Qian,[64] A. Quadt,[22,§] B. Quinn,[66] A. Rakitine,[42]

M. S. Rangel,[2] K. Ranjan,[28] P. N. Ratoff,[42] P. Renkel,[79] S. Reucroft,[63] P. Rich,[44] J. Rieger,[54] M. Rijssenbeek,[72] I. Ripp-Baudot,[19] F. Rizatdinova,[76] S. Robinson,[43] R. F. Rodrigues,[3] M. Rominsky,[75] C. Royon,[18] P. Rubinov,[50] R. Ruchti,[55] G. Safronov,[37] G. Sajot,[14] A. Sánchez-Hernández,[33] M. P. Sanders,[17] A. Santoro,[3] G. Savage,[50] L. Sawyer,[60] T. Scanlon,[43] D. Schaile,[25] R. D. Schamberger,[72] Y. Scheglov,[40] H. Schellman,[53] T. Schliephake,[26] C. Schwanenberger,[44] A. Schwartzman,[68] R. Schwienhorst,[65] J. Sekaric,[49] H. Severini,[75] E. Shabalina,[51] M. Shamim,[59] V. Shary,[18] A. A. Shchukin,[39] R. K. Shivpuri,[28] V. Siccardi,[19] V. Simak,[10] V. Sirotenko,[50] P. Skubic,[75] P. Slattery,[71] D. Smirnov,[55] G. R. Snow,[67] J. Snow,[74] S. Snyder,[73] S. Söldner-Rembold,[44] L. Sonnenschein,[17] A. Sopczak,[42] M. Sosebee,[78] K. Soustruznik,[9] B. Spurlock,[78] J. Stark,[14] J. Steele,[60] V. Stolin,[37] D. A. Stoyanova,[39] J. Strandberg,[64] S. Strandberg,[41] M. A. Strang,[69] E. Strauss,[72] M. Strauss,[75] R. Ströhmer,[25] D. Strom,[53] L. Stutte,[50] S. Sumowidagdo,[49] P. Svoisky,[55] A. Sznajder,[3] P. Tamburello,[45] A. Tanasijczuk,[1] W. Taylor,[6] J. Temple,[45] B. Tiller,[25] F. Tissandier,[13] M. Titov,[18] V. V. Tokmenin,[36] T. Toole,[61] I. Torchiani,[23] T. Trefzger,[24] D. Tsybychev,[72] B. Tuchming,[18] C. Tully,[68] P. M. Tuts,[70] R. Unalan,[65] L. Uvarov,[40] S. Uvarov,[40] S. Uzunyan,[52] B. Vachon,[6] P. J. van den Berg,[34] R. Van Kooten,[54] W. M. van Leeuwen,[34] N. Varelas,[51] E. W. Varnes,[45] I. A. Vasilyev,[39] M. Vaupel,[26] P. Verdier,[20] L. S. Vertogradov,[36] M. Verzocchi,[50] F. Villeneuve-Seguier,[43] P. Vint,[43] P. Vokac,[10] E. Von Toerne,[59] M. Voutilainen,[68,‖] R. Wagner,[68] H. D. Wahl,[49] L. Wang,[61] M. H. L. S. Wang,[50] J. Warchol,[55] G. Watts,[82] M. Wayne,[55] G. Weber,[24] M. Weber,[50] L. Welty-Rieger,[54] A. Wenger,[23,¶] N. Wermes,[22] M. Wetstein,[61] A. White,[78] D. Wicke,[26] G. W. Wilson,[58] S. J. Wimpenny,[48] M. Wobisch,[60] D. R. Wood,[63] T. R. Wyatt,[44] Y. Xie,[77] S. Yacoob,[53] R. Yamada,[50] M. Yan,[61] T. Yasuda,[50] Y. A. Yatsunenko,[36] K. Yip,[73] H. D. Yoo,[77] S. W. Youn,[53] J. Yu,[78] A. Zatserklyaniy,[52] C. Zeitnitz,[26] T. Zhao,[82] B. Zhou,[64] J. Zhu,[72] M. Zielinski,[71] D. Zieminska,[54] A. Zieminski,[54,**] L. Zivkovic,[70] V. Zutshi,[52] and E. G. Zverev[38]

(D0 Collaboration)

[1]*Universidad de Buenos Aires, Buenos Aires, Argentina*
[2]*LAFEX, Centro Brasileiro de Pesquisas Físicas, Rio de Janeiro, Brazil*
[3]*Universidade do Estado do Rio de Janeiro, Rio de Janeiro, Brazil*
[4]*Universidade Federal do ABC, Santo André, Brazil*
[5]*Instituto de Física Teórica, Universidade Estadual Paulista, São Paulo, Brazil*
[6]*University of Alberta, Edmonton, Alberta, Canada, Simon Fraser University, Burnaby, British Columbia, Canada, York University, Toronto, Ontario, Canada, and McGill University, Montreal, Quebec, Canada*
[7]*University of Science and Technology of China, Hefei, People's Republic of China*
[8]*Universidad de los Andes, Bogotá, Colombia*
[9]*Center for Particle Physics, Charles University, Prague, Czech Republic*
[10]*Czech Technical University, Prague, Czech Republic*
[11]*Center for Particle Physics, Institute of Physics, Academy of Sciences of the Czech Republic, Prague, Czech Republic*
[12]*Universidad San Francisco de Quito, Quito, Ecuador*
[13]*LPC, Université Blaise Pascal, CNRS/IN2P3, Clermont, France*
[14]*LPSC, Université Joseph Fourier Grenoble 1, CNRS/IN2P3, Institut National Polytechnique de Grenoble, France*
[15]*CPPM, IN2P3/CNRS, Université de la Méditerranée, Marseille, France*
[16]*LAL, Université Paris-Sud, IN2P3/CNRS, Orsay, France*
[17]*LPNHE, IN2P3/CNRS, Universités Paris VI and VII, Paris, France*
[18]*DAPNIA/Service de Physique des Particules, CEA, Saclay, France*
[19]*IPHC, Université Louis Pasteur et Université de Haute Alsace, CNRS/IN2P3, Strasbourg, France*
[20]*IPNL, Université Lyon 1, CNRS/IN2P3, Villeurbanne, France and Université de Lyon, Lyon, France*
[21]*III. Physikalisches Institut A, RWTH Aachen, Aachen, Germany*
[22]*Physikalisches Institut, Universität Bonn, Bonn, Germany*
[23]*Physikalisches Institut, Universität Freiburg, Freiburg, Germany*
[24]*Institut für Physik, Universität Mainz, Mainz, Germany*
[25]*Ludwig-Maximilians-Universität München, München, Germany*
[26]*Fachbereich Physik, University of Wuppertal, Wuppertal, Germany*
[27]*Panjab University, Chandigarh, India*
[28]*Delhi University, Delhi, India*
[29]*Tata Institute of Fundamental Research, Mumbai, India*
[30]*University College Dublin, Dublin, Ireland*
[31]*Korea Detector Laboratory, Korea University, Seoul, Korea*

[32]SungKyunKwan University, Suwon, Korea
[33]CINVESTAV, Mexico City, Mexico
[34]FOM-Institute NIKHEF and University of Amsterdam/NIKHEF, Amsterdam, The Netherlands
[35]Radboud University Nijmegen/NIKHEF, Nijmegen, The Netherlands
[36]Joint Institute for Nuclear Research, Dubna, Russia
[37]Institute for Theoretical and Experimental Physics, Moscow, Russia
[38]Moscow State University, Moscow, Russia
[39]Institute for High Energy Physics, Protvino, Russia
[40]Petersburg Nuclear Physics Institute, St. Petersburg, Russia
[41]Lund University, Lund, Sweden,
Royal Institute of Technology and Stockholm University, Stockholm, Sweden,
and Uppsala University, Uppsala, Sweden
[42]Lancaster University, Lancaster, United Kingdom
[43]Imperial College, London, United Kingdom
[44]University of Manchester, Manchester, United Kingdom
[45]University of Arizona, Tucson, Arizona 85721, USA
[46]Lawrence Berkeley National Laboratory and University of California, Berkeley, California 94720, USA
[47]California State University, Fresno, California 93740, USA
[48]University of California, Riverside, California 92521, USA
[49]Florida State University, Tallahassee, Florida 32306, USA
[50]Fermi National Accelerator Laboratory, Batavia, Illinois 60510, USA
[51]University of Illinois at Chicago, Chicago, Illinois 60607, USA
[52]Northern Illinois University, DeKalb, Illinois 60115, USA
[53]Northwestern University, Evanston, Illinois 60208, USA
[54]Indiana University, Bloomington, Indiana 47405, USA
[55]University of Notre Dame, Notre Dame, Indiana 46556, USA
[56]Purdue University Calumet, Hammond, Indiana 46323, USA
[57]Iowa State University, Ames, Iowa 50011, USA
[58]University of Kansas, Lawrence, Kansas 66045, USA
[59]Kansas State University, Manhattan, Kansas 66506, USA
[60]Louisiana Tech University, Ruston, Louisiana 71272, USA
[61]University of Maryland, College Park, Maryland 20742, USA
[62]Boston University, Boston, Massachusetts 02215, USA
[63]Northeastern University, Boston, Massachusetts 02115, USA
[64]University of Michigan, Ann Arbor, Michigan 48109, USA
[65]Michigan State University, East Lansing, Michigan 48824, USA
[66]University of Mississippi, University, Mississippi 38677, USA
[67]University of Nebraska, Lincoln, Nebraska 68588, USA
[68]Princeton University, Princeton, New Jersey 08544, USA
[69]State University of New York, Buffalo, New York 14260, USA
[70]Columbia University, New York, New York 10027, USA
[71]University of Rochester, Rochester, New York 14627, USA
[72]State University of New York, Stony Brook, New York 11794, USA
[73]Brookhaven National Laboratory, Upton, New York 11973, USA
[74]Langston University, Langston, Oklahoma 73050, USA
[75]University of Oklahoma, Norman, Oklahoma 73019, USA
[76]Oklahoma State University, Stillwater, Oklahoma 74078, USA
[77]Brown University, Providence, Rhode Island 02912, USA
[78]University of Texas, Arlington, Texas 76019, USA
[79]Southern Methodist University, Dallas, Texas 75275, USA
[80]Rice University, Houston, Texas 77005, USA
[81]University of Virginia, Charlottesville, Virginia 22901, USA
[82]University of Washington, Seattle, Washington 98195, USA
(Received 12 March 2008; published 29 July 2008)

We report the results of a search for a narrow resonance decaying into two photons in 1.1 fb^{-1} of data collected by the D0 experiment at the Fermilab Tevatron Collider during the period 2002–2006. We find no evidence for such a resonance and set a lower limit on the mass of a fermiophobic Higgs boson of $m_{h_f} > 100$ GeV at the 95% C.L. This exclusion limit exceeds those obtained in previous searches at the Fermilab Tevatron and covers a significant region of the parameter space $B(h_f \to \gamma\gamma)$ vs m_{h_f} which was not accessible at the CERN Large Electron-Positron Collider.

DOI: 10.1103/PhysRevLett.101.051801 PACS numbers: 14.80.Cp, 12.60.Fr, 13.85.Rm

In the standard model (SM), the Higgs field is responsible for both electroweak symmetry breaking and generating elementary fermion masses. While the SM describes our world at current experimentally accessible energies, the exact mechanism for electroweak symmetry breaking remains a mystery.

Diphoton decays of the Higgs boson are suppressed at tree level, and in the SM such decays have a very small branching fraction: 10^{-3}–10^{-4}. However, in a more general framework where the parameter content of the theory is richer, such decays can be enhanced. In the situation where the Higgs-fermion couplings are substantially suppressed, the full decay width of the Higgs boson would be shared mostly among the WW, ZZ, and $\gamma\gamma$ decay modes. Such a scenario, the so-called "fermiophobic" Higgs boson, arises in a variety of models, e.g., [1–3]. In all of these cases, for masses $m_h < 100$ GeV, the Higgs boson dominantly decays to photon pairs.

Experimental searches for fermiophobic Higgs bosons (h_f) at the CERN Large Electron-Positron (LEP) Collider and the Fermilab Tevatron Collider have yielded negative results. Mass limits have been set in a benchmark model that assumes that the coupling $h_f VV$ ($V \equiv W^\pm, Z$) has the same strength as in the SM and that all fermion branching ratios (B) are exactly zero. Combination of results obtained by the LEP Collaborations [4–7] using the process $e^+e^- \to h_f Z$, $h_f \to \gamma\gamma$, yielded the lower bound $m_h > 109.7$ GeV at the 95% C.L. [8]. In run I of the Tevatron, lower limits on m_{h_f} from the D0 and CDF Collaborations are, respectively, 78.5 [9] and 82 GeV [10], using the processes $q\bar{q}' \to V^* \to h_f V$, $h_f \to \gamma\gamma$, with the dominant contribution coming from $V = W^\pm$.

In this Letter, we perform a search for the inclusive production of diphoton final states via the Higgsstrahlung and vector boson fusion processes: $p\bar{p} \to h_f V \to \gamma\gamma + X$ and $p\bar{p} \to VV \to h_f \to \gamma\gamma + X$, respectively. The total integrated luminosity of the data used for this search is 1.10 ± 0.07 fb^{-1}.

The D0 detector comprises a central tracking system in a 2 T superconducting solenoid, a liquid-argon/uranium sampling calorimeter, and a muon spectrometer. The calorimeter consists of a central section covering the pseudorapidity range $|\eta| < 1.1$, which is defined as $\eta \equiv -\ln[\tan(\theta/2)]$, where θ is the polar angle with respect to the proton beam direction, and two end caps extending coverage to $|\eta| < 4.2$, each housed in a separate cryostat. The electromagnetic (EM) section of the calorimeter has four layers with longitudinal depths of $2X_0$, $2X_0$, $7X_0$, and $10X_0$ that provide full containment of EM particles (photons and electrons). The calorimeter layers have transverse segmentation of $\delta\phi \times \delta\eta = 0.1 \times 0.1$ (where ϕ is the azimuthal angle), except in the third layer, where it is 0.05×0.05, which allows for accurate determination of the position of EM particles. Immediately before the inner layer of the central EM calorimeter, there is a central preshower detector (CPS) formed of $2X_0$ of absorber followed by several layers of scintillating strips with embedded wavelength-shifting fibers. A complete description of the D0 detector can be found in Ref. [11].

We select events that satisfy single EM triggers which become fully efficient for EM showers with transverse momentum $p_T > 30$ GeV. Photons and electrons are identified in two steps: the selection of EM clusters and their subsequent separation into those caused by photons and those caused by electrons. EM clusters are selected from calorimeter clusters by requiring that (i) at least 97% of the energy be deposited in the EM section of the calorimeter, (ii) the calorimeter isolation be less than 0.07 (isolation is defined as $[E_{\mathrm{tot}}(0.4) - E_{\mathrm{EM}}(0.2)]/E_{\mathrm{EM}}(0.2)$, where $E_{\mathrm{tot}}(0.4)$ is the total shower energy in a cone of radius $R = \sqrt{(\Delta\eta)^2 + (\Delta\phi)^2} = 0.4$ and $E_{\mathrm{EM}}(0.2)$ is the EM energy in a cone with $R = 0.2$), (iii) the transverse, energy-weighted shower width be less than 0.04 rad (i.e., consistent with an EM shower profile), and (iv) the scalar p_T sum of all tracks originating from the primary vertex in an annulus of $0.05 < R < 0.4$ around the cluster be less than 2 GeV. The cluster is then defined as an electron if there is a reconstructed track (or electronlike pattern of hits in the tracker) associated with it and a photon otherwise. We also consider EM jets (jets with a leading π^0 or η) defined as EM clusters that pass all cuts required for photon candidates except the track isolation requirement. We will refer to them as "j" or "jet." We select events that have at least two photons in the central calorimeter ($|\eta| < 1.1$) with transverse momenta $p_T > 25$ GeV. Events are required to have the primary vertex within 60 cm of the geometrical center of the detector. Identification of the primary vertex in the event is important, as it affects the calculation of the p_T of a photon candidate and its track isolation. Despite the fact that photons do not leave tracks, the probability to reconstruct a primary vertex is high, 99.5%, due to the underlying event activity.

The Higgs boson produced in the models considered has higher transverse momentum $q_T^{\gamma\gamma}$ than most of the background. Therefore, we select events with $q_T^{\gamma\gamma} > 35$ GeV. For simplicity, we choose a fixed cut value which is below the optimum for Higgs boson masses starting from 70 GeV. After all selection criteria, we are left with 196 (1509) diphoton events with $q_T^{\gamma\gamma} > 35$ ($q_T^{\gamma\gamma} < 35$) GeV for invariant masses above 65 GeV.

The dominant background comes from direct diphoton production (DDP) processes. The other major background comes from events in which jets are misidentified as photons: γj processes, where a quark or a gluon fragmented into an energetic π^0 or η and is reconstructed as a photon,

and the multijet background, where two jets are misidentified as photons.

Another source of diphoton background comes from events in which electrons are misidentified as photons: the decay of a Z boson where electrons are reconstructed as photons if there are no associated tracks, and processes with one real electron coming from the decay of a $W^{\pm}$ boson produced in association with a real photon or a jet misreconstructed as a photon. The veto of electronlike patterns of hits in the tracker reduces electron backgrounds by a factor of 5 while keeping the photon efficiency high. We measure that $(91 \pm 3)\%$ of photon candidates in $Z/\gamma^* \rightarrow e^+e^-\gamma$ data satisfy the antitrack activity requirement. The contribution of events with one or two real electrons is obtained by applying the probability for an electron to fail the track requirement and be reconstructed as a photon ($1.5^{+3.0}_{-1.5}\%$) to the Z boson, Drell-Yan, and $W^{\pm} + X$ event yields. This background is estimated to be less than one event.

We estimate the relative contributions of the $\gamma\gamma$, γj, and jj backgrounds, where j corresponds to a jet reconstructed as a photon, using the difference in the energy-weighted width of the energy deposition in the CPS $\sigma_E^{\rm CPS}$. The width is generally narrower for photons than for jets. We construct one-dimensional templates as a function of $x = \sigma_E^{\rm CPS}$ for photons [$G(x)$] and jets [$J(x)$]. The $G(x)$ is constructed using radiative $Z/\gamma^* \rightarrow \ell^+\ell^-\gamma$ ($\ell = e, \mu$) decays in data, and the $J(x)$ is taken from the jj data sample. From these we construct two-dimensional profiles for the three components $\gamma\gamma$, γj, and jj, as follows: $GG(x, y) = G(x)G(y)$, $GJ(x, y) = 0.5[G(x)J(y) + J(x)G(y)]$, and $JJ(x, y) = J(x)J(y)$. Further, using these two-dimensional templates we construct a fitting function: $c_0[GG(x, y) + c_1 JJ(x, y) + c_2 GJ(x, y)]$. The parameters are chosen so that c_0 is equal to the number of $\gamma\gamma$ events and responsible for the overall normalization, and c_1 and c_2 determine the contributions of jj and γj events relative to $\gamma\gamma$.

For the diphoton candidate data sample, we make a two-dimensional distribution of $\sigma_E^{\rm CPS}$. For each event we randomly decide whether the leading photon is plotted along the x or the y axis. We fit this distribution with the function defined above to determine the individual components: $c_0 = 131 \pm 22 \pm 7$ events, $c_1 = 0.35 \pm 0.19 \pm 0.06$, and $c_2 = 0.13 \pm 0.28 \pm 0.13$, where the first error is the statistical error of the fit and the second is the systematic uncertainty in the shape of the photon template obtained from variations of the fitting range, binning of the templates, and the source of the photon template.

The next step is to use the derived fractions to model the mass distribution of the diphoton candidate data. For this we need three mass templates: $T_{\gamma\gamma}$, $T_{\gamma j}$, and T_{jj}. We take $T_{\gamma\gamma}$ from PYTHIA Monte Carlo (MC) calculations [12] corrected for detector effects and reweighted with the K factor derived from RESBOS [13] to account for the (next-to-)next-to-leading order [NLO (NNLO)] effects. The other two templates are taken from γj and jj samples, where we relax the calorimeter isolation, EM fraction, and energy-weighted shower width requirements in the definition of a jet in order to increase statistics in these templates. We verify that relaxing the requirements does not alter the kinematics of the sample. We also correct the γj mass template for the admixture of jj events. We construct the background mass spectrum assuming the functional form $N_{\gamma\gamma}(T_{\gamma\gamma} + c_1 T_{jj} + c_2 T_{\gamma j})$, where $T_{\gamma\gamma}$, $T_{\gamma j}$, and T_{jj} are mass distributions normalized to one (see Fig. 1), c_1 and c_2 are taken from the CPS fit above, and $N_{\gamma\gamma}$ is the expected number of DDP events from the MC calculations. For the measured luminosity, we estimate $N_{\gamma\gamma} = 113 \pm 3.5(\text{stat}) \pm 24(\text{syst})$ events, which is in agreement with the $c_0 = 131 \pm 22 \pm 7$ events derived from data. While these numbers agree within the theoretical and experimental uncertainties, we choose to normalize the number of background events to the total number of events observed in the data (normalization events are counted outside of the signal region, defined as a ± 5 GeV window in diphoton mass centered at each hypothesized m_{h_f} value). By doing so, we eliminate most of the background uncertainties, e.g., luminosity and renormalization scale.

Figure 2 shows the mass distributions in data with overlaid background predictions. The shaded regions correspond to the expected background error bands. The inner band represents the statistical uncertainty of the mass templates, while the outer corresponds to the systematics due to variation in the one-dimensional $\sigma_E^{\rm CPS}$ templates. We assign an additional 100% uncertainty that includes any possible change in the shape of the mass templates due to the relaxed definition of a jet.

Signal events are generated for a range of mass points from 70 to 150 GeV in 10 GeV steps. We use the PYTHIA event generator followed by a detailed GEANT-based [14] simulation of the D0 detector. The signal efficiencies $\epsilon^{\rm signal}$

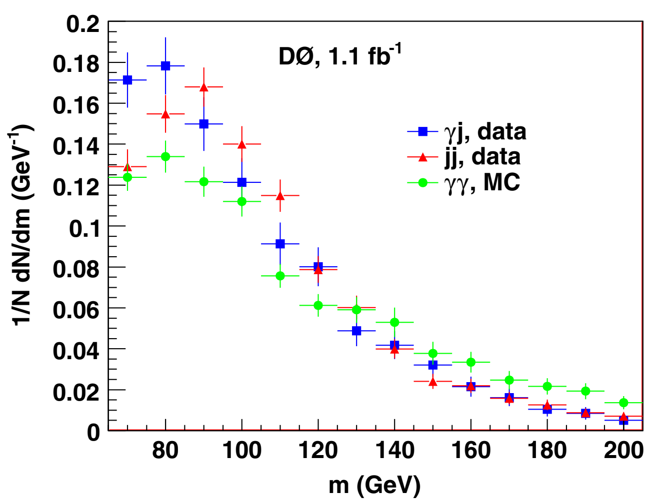

FIG. 1 (color online). Normalized distributions of the invariant mass m of $\gamma\gamma$ (circles), γj (squares), and jj (triangles).

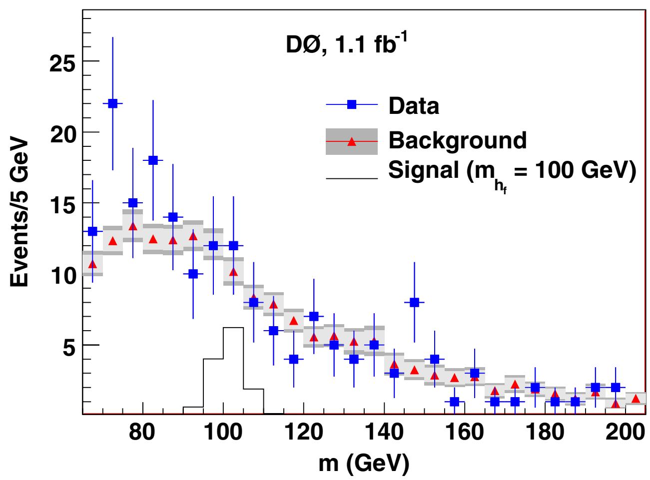

FIG. 2 (color online). Diphoton mass distribution of the data (squares), with the overlaid background prediction (triangles), and the expected signal distribution for $m_{h_f} = 100$ GeV in the benchmark model. The inner background error band corresponds to the statistical uncertainty, and the outer is a linear sum of the statistical and the systematic uncertainties.

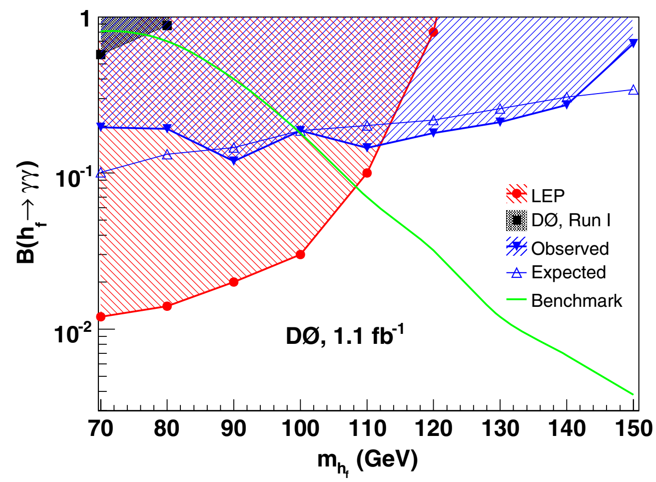

FIG. 3 (color online). $B(h_f \to \gamma\gamma)$ limits as a function of the Higgs mass. The theoretical $B(h_f \to \gamma\gamma)$ curve for the benchmark model as well as the observed $B(h_f \to \gamma\gamma)$ limits from D0 run I and LEP are overlaid. The shaded regions correspond to the excluded values of the branching ratio.

are derived from the MC calculations. Table I lists signal efficiencies after correction for trigger inefficiency and scaling by the ratio of efficiencies in data and MC calculations (≈95% per photon) obtained from the electron reconstruction efficiency in $Z \to e^+e^-$ events. Note that the photon requirements are chosen in such a way that the MC calculation correctly reproduces differences between electrons and photons as confirmed in $Z \to e^+e^-\gamma$ events. Table I also shows the number of observed diphoton candidate events in data in 10 GeV mass windows and the corresponding background estimates with associated uncertainties. The width of the mass peak is dominated by the detector resolution and varies between 2.8 and 5.2 GeV. The size of the optimal mass window varies between 8 and 15 GeV, but for simplicity we use a fixed value of 10 GeV. The acceptance of the mass window cuts varies between 94% and 66% for $m_{h_f} = 70$–150 GeV. In the same table, we provide the theoretical benchmark branching ratio $B(h \to \gamma\gamma)$ [15] and the NLO cross section $\sigma_h^{\rm NLO}$ for the sum of the signal processes $p\bar{p} \to VV \to h_f$ and $p\bar{p} \to h_f V$ obtained with VV2H and V2HV [16].

We perform a counting experiment in the 10 GeV mass windows, and, in the absence of an excess of diphoton events, we set an upper limit on the product of the Higgs boson production cross section and diphoton branching ratio $\sigma_{h_f} B(h_f \to \gamma\gamma)$ at 95% C.L. Limits are calculated using the modified frequentist CL_S method [17]. Table I shows the expected and observed limits. The choice of the fixed size mass window, which is slightly different from the optimal one for Higgs masses below and above 100 GeV, slightly increases the expected excluded cross section. The present study excludes fermiophobic Higgs bosons of mass up to 100 GeV at the 95% C.L. This is the most stringent limit to date at a hadron collider. In Fig. 3, we present our results as limits on the branching ratio in the parameter

TABLE I. Input data for limit calculation and 95% C.L. limits on cross section times branching fraction. Quoted are the total uncertainties that are used in the limit calculation.

				$\sigma(p\bar{p} \to h_f + X) \cdot B(h_f \to \gamma\gamma)$ (pb)				
m_{h_f} (GeV)	Data	Background	$\epsilon^{\rm signal}$ (%)	Expected limit	Observed limit	Run I limit	$\sigma_h^{\rm NLO}$ (pb)	$B(h_f \to \gamma\gamma)$
70	35	24.5 ± 4.6	6.9 ± 0.5	0.15	0.29	0.46	1.5	0.81
80	33	27.2 ± 5.0	7.9 ± 0.6	0.14	0.20	0.44	1.0	0.70
90	24	27.4 ± 5.4	9.8 ± 0.8	0.11	0.089	0.37	0.75	0.41
100	24	23.7 ± 4.8	10.3 ± 0.8	0.10	0.10	0.35	0.55	0.18
110	14	17.7 ± 4.4	11.2 ± 0.9	0.085	0.061	0.34	0.42	0.062
120	11	13.4 ± 3.7	11.3 ± 0.9	0.070	0.058	0.33	0.32	0.028
130	9	11.7 ± 3.3	11.2 ± 0.9	0.065	0.053	0.33	0.25	0.019
140	8	9.5 ± 2.8	11.7 ± 0.9	0.058	0.052	0.32	0.19	0.0061
150	12	6.3 ± 2.1	11.7 ± 0.9	0.051	0.10	0.32	0.15	0.0020

space $B(h_f \to \gamma\gamma)$ vs m_{h_f} obtained from a ratio of the above limits and $\sigma_h^{\rm NLO}$. The regions above the experimental points correspond to the excluded values of the branching ratio.

In summary, this study significantly improves the LEP limits at intermediate mass values, e.g., by more than a factor of 4 at $m_{h_f} = 120$ GeV, and extends sensitivity into the region not accessible at LEP: $m_{h_f} > 130$ GeV.

We thank the staffs at Fermilab and collaborating institutions and acknowledge support from the DOE and NSF (USA); CEA and CNRS/IN2P3 (France); FASI, Rosatom, and RFBR (Russia); CNPq, FAPERJ, FAPESP, and FUNDUNESP (Brazil); DAE and DST (India); Colciencias (Colombia); CONACyT (Mexico); KRF and KOSEF (Korea); CONICET and UBACyT (Argentina); FOM (The Netherlands); STFC (United Kingdom); MSMT and GACR (Czech Republic); CRC Program, CFI, NSERC, and WestGrid Project (Canada); BMBF and DFG (Germany); SFI (Ireland); The Swedish Research Council (Sweden); CAS and CNSF (China); and the Alexander von Humboldt Foundation.

*Visitor from Augustana College, Sioux Falls, SD, USA.
†Visitor from The University of Liverpool, Liverpool, United Kingdom.
‡Visitor from ICN-UNAM, Mexico City, Mexico.
§Visitor from II. Physikalisches Institut, Georg-August-University, Göttingen, Germany.
‖Visitor from Helsinki Institute of Physics, Helsinki, Finland.
¶Visitor from Universität Zürich, Zürich, Switzerland.
**Deceased.

[1] H. E. Haber, G. L. Kane, and T. Sterling, Nucl. Phys. **B161**, 493 (1979); J. F. Gunion, R. Vega, and J. Wudka, Phys. Rev. D **42**, 1673 (1990); J. L. Basdevant, E. L. Berger, D. Dicus, C. Kao, and S. Willenbrock, Phys. Lett. B **313**, 402 (1993); V. Barger, N. G. Deshpande, J. L. Hewett, and T. G. Rizzo, arXiv:hep-ph/9211234; P. Bamert and Z. Kunszt, Phys. Lett. B **306**, 335 (1993); A. G. Akeroyd, Phys. Lett. B **368**, 89 (1996); M. C. Gonzalez-Garcia, S. M. Lietti, and S. F. Novaes, Phys. Rev. D **57**, 7045 (1998); A. Barroso, L. Brucher, and R. Santos, Phys. Rev. D **60**, 035005 (1999); L. Brucher and R. Santos, Eur. Phys. J. C **12**, 87 (2000).
[2] B. Dobrescu, Phys. Rev. D **63**, 015004 (2000); B. Dobrescu, G. Landsberg, and K. Matchev, Fermilab Report No. FERMILAB-PUB-99/324-T.
[3] L. Hall and C. Kolda, Phys. Lett. B **459**, 213 (1999); H. Cheng, B. A. Dobrescu, and C. T. Hill, Nucl. Phys. **B589**, 249 (2000).
[4] A. Heister *et al.* (ALEPH Collaboration), Phys. Lett. B **544**, 16 (2002).
[5] P. Abreu *et al.* (DELPHI Collaboration), Phys. Lett. B **507**, 89 (2001); Eur. Phys. J. C **35**, 313 (2004).
[6] P. Achard *et al.* (L3 Collaboration), Phys. Lett. B **534**, 28 (2002); **568**, 191 (2003).
[7] G. Abbiendi *et al.* (OPAL Collaboration), Phys. Lett. B **544**, 44 (2002).
[8] A. Rosca, arXiv:hep-ph/0212038v1.
[9] B. Abbott *et al.* (D0 Collaboration), Phys. Rev. Lett. **82**, 2244 (1999).
[10] T. Affolder *et al.* (CDF Collaboration), Phys. Rev. D **64**, 092002 (2001).
[11] V. M. Abazov *et al.* (D0 Collaboration), Nucl. Instrum. Methods Phys. Res., Sect. A **565**, 463 (2006).
[12] T. Sjöstrand *et al.*, arXiv:hep-ph/0308153.
[13] C. Balazs and C. P. Yuan, Phys. Rev. D **56**, 5558 (1997); C. Balazs *et al.*, Phys. Rev. D **76**, 013009 (2007); C. Balazs *et al.*, Phys. Lett. B **637**, 235 (2006).
[14] R. Brun and F. Carminati, CERN Program Library Long Writeup Report No. W5013, 1993 (unpublished).
[15] S. Mrenna and J. Wells, Phys. Rev. D **63**, 015006 (2000).
[16] M. Spira, Comput. Phys. Commun. **108**, 56 (1998).
[17] T. Junk, Nucl. Instrum. Methods Phys. Res., Sect. A **434**, 435 (1999).